Eur. Phys. J. B **10**, 573–582 (1999)

THE EUROPEAN PHYSICAL JOURNAL B

EDP Sciences

The Nagel-Schreckenberg model revisited

A. Schadschneider[a]

Institut für Theoretische Physik, Universität zu Köln, 50937 Köln, Germany

Received 5 February 1999

Abstract. The Nagel-Schreckenberg model is a simple cellular automaton for a realistic description of single-lane traffic on highways. For the case $v_{\max} = 1$ the properties of the stationary state can be obtained exactly. For the more relevant case $v_{\max} > 1$, however, one has to rely on Monte Carlo simulations or approximative methods. Here we study several analytical approximations and compare with the results of computer simulations. The role of the braking parameter p is emphasized. It is shown how the local structure of the stationary state depends on the value of p. This is done by combining the results of computer simulations with those of the approximative methods.

PACS. 02.50.Ey Stochastic processes – 05.60.-k Transport processes – 89.40.+k Transportation

1 Introduction

Cellular automata (CA) do not only serve as simple model systems for the investigation of problems in statistical mechanics, but they also have numerous applications to "real" problems [1]. Therefore it is not surprising that in recent years CA have become quite popular for the simulation of traffic flow (see *e.g.* [2,3]).

CA are – by design – ideal for large-scale computer simulations. On the other hand, analytical approaches for the description of CA are notoriously difficult. This is mainly due to the discreteness and the use of a parallel updating scheme (which introduces "non-locality" into the dynamics). In addition, these models are defined through dynamical rules (*e.g.* transition probabilities) and usually one does not have a "Hamiltonian" description. Therefore standard methods are not applicable. Furthermore, one has to deal with systems which do not satisfy the detailed balance condition.

However, there is a need for exact solutions or, at least, for good approximations. These results as well as other exact statements may help to greatly reduce the need for computer resources. The interpretation of simulation data is often difficult because of the "numerical noise" and finite-size effects. Even in the cases where an exact solution is not possible, a combination of analytical and numerical methods might provide better insights. This is especially true for non-equilibrium systems where only a few exact or general results exist which could serve as a guideline.

In recent years, several analytical approximation methods for the Nagel-Schreckenberg model [4] for single-lane highway traffic have been proposed [5–8]. All of these approximations yield the exact result for the stationary state in the case $v_{\max} = 1$. However, these investigations focused on the so-called fundamental diagram, *i.e.* the flow-density relation. Here we will reinvestigate these approximations and calculate further quantities of interest in order to determine the accuracy. We will also discuss several limits and emphasize the effect of the braking probability p. We focus on the effect of p on the microscopic structure of the stationary state. Such microscopic characterizations have recently been used successfully for the asymmetric exclusion process [9,10]. Apart from $v_{\max} = 1$ here only the case of $v_{\max} = 2$ is investigated since one does not expect a qualitatively different behaviour for $v_{\max} \geq 2$ [6].

The paper is organized as follows: First we will briefly recall the definition of the Nagel-Schreckenberg model in Section 2 and the different analytical approximations in Section 3. In Section 4 several physical quantities, *e.g.* the fundamental diagram, headway and jam-size distributions and correlation lengths, are calculated using the analytical results. In Section 5 the predictions of the approximations are compared with each other and with results from computer simulations. The local structure of the stationary state is investigated as a function of the randomization p. In the final Section 6 a summary of the results together with our conclusion are given.

2 The Nagel-Schreckenberg model

The Nagel-Schreckenberg (NaSch) model [4] is a probabilistic cellular automaton. Space and time are discrete and hence also the velocities. The road is divided into cells. The length of a cell is determined by the front-bumper to front-bumper distance of cars in the densest jam and is usually taken to be 7.5 m. Each cell can either

[a] e-mail: as@thp.uni-koeln.de

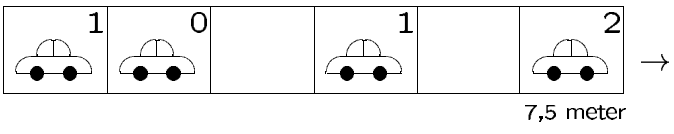

Fig. 1. Configuration in the Nagel-Schreckenberg model. The number in the upper right corner gives the velocity of the car.

be empty or occupied by just one car. The state of car j ($j = 1, \ldots, N$) is characterised by an internal parameter v_j ($v_j = 0, 1, \ldots, v_{\max}$), the instantaneous velocity of the vehicle. In order to obtain the state of the system at time $t+1$ from the state at time t, one has to apply the following four rules to all cars at the same time (parallel dynamics) [4]:

R1 Acceleration: $v_j(t+1/3) = \min(v_j(t)+1, v_{\max})$
R2 Braking: $v_j(t+2/3) = \min(d_j(t), v_j(t+1/3))$
R3 Randomization: $v_j(t+1) \stackrel{p}{=} \max(v_j(t+2/3)-1, 0)$ with probability p
R4 Driving: car j moves $v_j(t+1)$ cells.

Here $d_j(t)$ denotes the number of empty cells in front of car j, *i.e.* the so-called headway. For $v_{\max} = 5$ a calibration of the model shows that each timestep $t \to t+1$ corresponds to approximately 1 s in real time [4]. For simplicity we will consider only periodic boundary conditions so that the number of cars is conserved. The maximum velocity $v_{\max}$ can be interpreted as a speed limit and is therefore taken to be identical for all cars. Figure 1 shows a typical configuration. Throughout the paper we will assume that the cars move from left to right.

The four steps have simple interpretations. Step R1 means that every driver wants to drive as fast as possible or allowed. Step R2 avoids crashes between the vehicles. The randomization step R3 takes into account several effects, *e.g.* road conditions (*e.g.* slope, weather) or psychological effects (*e.g.* velocity fluctuations in free traffic). An important consequence of this step is the introduction of overreactions at braking which are crucial for the occurrence of spontaneous jam formation. Finally, step R4 is the actual motion of the vehicles.

The NaSch model is a minimal model in the sense that all four steps R1-R4 are necessary to reproduce the basic properties of real traffic. For more complex situations (*e.g.* 2-lane traffic [11] or city traffic [12]) additional rules have to be formulated.

3 Analytical methods

In this section several analytical approaches which have been used for the description of the NaSch model are reviewed. The simplest, a mean-field (MF) theory, completely neglects correlations. Since MF theory turned out to be inadequate even for the fundamental diagram, improved methods have been developed which allow to take into account short-range correlations exactly. All methods described here are *microscopic* theories since macroscopic theories are not able to describe the NaSch model properly. However, they are extremely useful and accurate for special variants of the NaSch model, *e.g.* the VDR model [13] in the slow-to-start limit.

In the following the analytical approaches are discussed briefly for the cases $v_{\max} = 1$ and $v_{\max} = 2$. All methods other than MF theory are exact for $v_{\max} = 1$. For $v_{\max} = 2$, on the other hand, they are only approximations.

Applications of the analytical methods to the calculation of physical quantities, *e.g.* the fundamental diagram, jam-size distributions and correlation lengths, are given in Section 4.

3.1 Mean-field theory

The simplest analytical approach to the NaSch model is a (microscopic) mean-field (MF) theory [6]. Here one considers the density $c_v(j,t)$ of cars with velocity v at site j and time t. In the MF approach, correlations between sites are completely neglected.

For $v_{\max} = 1$ the MF equations for the stationary state ($t \to \infty$) read [6]:

$$c_0 = (c + pd)c, \tag{1}$$
$$c_1 = \bar{p}cd \tag{2}$$

with $c = c_0 + c_1$, $d = 1 - c$ and $\bar{p} = 1 - p$. The flow is simply given by $f_{\mathrm{MF}}(c) = c_1$.

For random-sequential dynamics[1] the MF approach is known to be exact for $v_{\max} = 1$ [4]. For parallel dynamics, however, MF theory underestimates the flow considerably (see Sect. 4.1).

For $v_{\max} = 2$ the rate equations for the densities are given by [6]

$$c_0 = (c + pd)c_0 + (1 + pd)c(c_1 + c_2), \tag{3}$$
$$c_1 = d\left[\bar{p}c_0 + (\bar{p}c + pd)(c_1 + c_2)\right], \tag{4}$$
$$c_2 = \bar{p}d^2(c_1 + c_2). \tag{5}$$

The solution is given by

$$c_0 = \frac{(1+pd)c^2}{1-pd^2},$$
$$c_1 = \frac{\bar{p}(1-\bar{p}d^2)dc}{1-pd^2}, \tag{6}$$
$$c_2 = \frac{\bar{p}^2 d^3 c}{1-pd^2},$$

and the flux can be calculated using $f_{\mathrm{MF}}(c) = c_1 + 2c_2$. Again the flow is underestimated considerably (see Sect. 4.1). This is true for arbitrary $v_{\max}$. The general form of the MF equations can be found in [6].

[1] In random-sequential dynamics in each timestep a cell which is updated is picked at random.

3.2 Cluster approximation

The cluster approximation [5,6] is a systematic improvement of MF theory which takes into account short-ranged correlations between the cells. In the n-cluster approximation a cluster of n neighbouring cells is treated exactly. The cluster is then coupled to the rest of the system in a self-consistent way. Related approximations have already been used (under different names) for other models [14–17].

In order to simplify the description, we sometimes choose a slightly different update-ordering R2-R3-R4-R1 instead of R1-R2-R3-R4, *i.e.* we look at the system after the acceleration step. Then there are no cars with $v = 0$ and effectively we have to deal with one equation less. In the following we will use occupation variables τ_j where $\tau_j = 0$, if cell j is empty, and $\tau_j = v$, if cell j is occupied by a car with velocity v. The change of the ordering has to be taken into account in the calculation of observables. The flow is given by $f(c) = \bar{p}P(1,0)$.

For an $n-$cluster of n consecutive cells with state variables $\boldsymbol{\tau}_j^{(n)}(t) = (\tau_j(t), \ldots, \tau_{j+n-1}(t))$ at time t it is straightforward to derive an exact evolution equation for the cluster probability $P(\tau_j(t), \ldots, \tau_{j+n-1}(t))$. One has to take into account that cars can enter the cluster from one of the $v_{\max}$ cells to the left of the cluster and can leave the cluster to one of the $v_{\max}$ cells to the right. Therefore the state $\boldsymbol{\tau}_j^{(n)}(t+1)$ of a cluster depends not only on its state $\boldsymbol{\tau}_j^{(n)}$ at time t, but also on the neighbouring cells $(\tau_{j-v_{\max}}(t), \ldots, \tau_{j-1}(t))$ and $(\tau_{j+n}(t), \ldots, \tau_{j+n+v_{\max}-1}(t))$.

In the stationary state the master equation for cluster $\boldsymbol{\tau}^{(n)} = (\tau_j, \ldots, \tau_{j+n-1})$ of n cells has the following structure:

$$P(\boldsymbol{\tau}^{(n)}) = \sum_{\boldsymbol{\tau}^{(n+2v_{\max})}} W(\boldsymbol{\tau}^{(n+2v_{\max})} \to \boldsymbol{\tau}^{(n)}) P(\boldsymbol{\tau}^{(n+2v_{\max})}) \tag{7}$$

where $\boldsymbol{\tau}^{(n+2v_{\max})} = (\tau_{j-v_{\max}}, \ldots, \tau_{j+n+v_{\max}-1})$. The transition probabilities $W(\boldsymbol{\tau}^{(n+2v_{\max})} \to \boldsymbol{\tau}^{(n)})$ have to be determined from the rules R1–R4. Note that the master equation for $n-$clusters involves $(n+2v_{\max})-$clusters. If the stationary state is translation-invariant the probabilities $P(\tau_j \ldots, \tau_{j+n-1})$ are independent of j.

In order to obtain a closed set of equations one has to express the $(n+2v_{\max})-$clusters through the $n-$cluster probabilities. At this point some approximation has to be made. Usual one uses a factorization into products of $n-$clusters. We illustrate this for $v_{\max} = 2$ and $n = 3$ (see Fig. 2):

$$\begin{aligned} P(\boldsymbol{\tau}^{(5)}) = {} & P(\tau_{j-2}|\underline{\tau_{j-1}, \tau_j}) P(\tau_{j-1}|\underline{\tau_j, \tau_{j+1}}) \\ & \times P(\tau_j, \tau_{j+1}, \tau_{j+2}) \\ & \times P(\underline{\tau_{j+1}, \tau_{j+2}}|\tau_{j+3}) P(\underline{\tau_{j+2}, \tau_{j+3}}|\tau_{j+4}) \end{aligned} \tag{8}$$

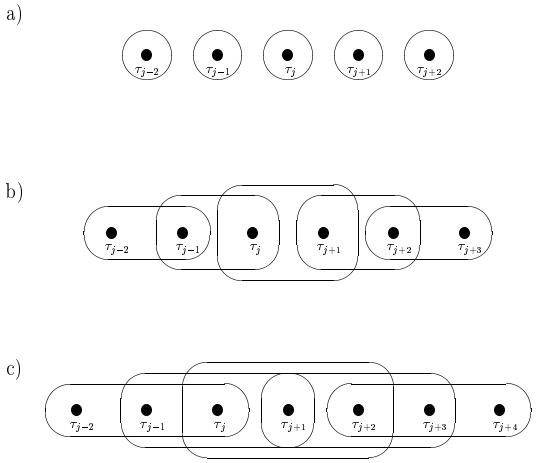

Fig. 2. Graphical representation of the $n-$cluster approximation for a) $n = 1$ (*i.e.* mean-field theory), b) $n = 2$, and c) $n = 3$. Shown is the central $n-$cluster starting at site j and all clusters which have to be taken into account in the master equation (7) for $v_{\max} = 2$.

with the conditional probabilities

$$P(\tau_1|\underline{\tau_2, \ldots, \tau_n}) = \frac{P(\tau_1, \ldots, \tau_n)}{\sum_\tau P(\tau, \tau_2, \ldots, \tau_n)}, \tag{9}$$

$$P(\underline{\tau_1, \ldots, \tau_{n-1}}|\tau_n) = \frac{P(\tau_1, \ldots, \tau_n)}{\sum_\tau P(\tau_1, \ldots, \tau_{n-1}, \tau)}. \tag{10}$$

If we denote the probability to find the system in a configuration $(\tau_1, \ldots, \tau_L)$ by $P(\tau_1, \ldots, \tau_L)$ the 1-cluster approximation means a simple factorization

$$P(\tau_1, \ldots, \tau_L) = \prod_{j=1}^{L} P(\tau_j). \tag{11}$$

This is nothing but the mean-field theory of Section 3.1. For the 2-cluster approximation one has a factorization of the form

$$P(\tau_1, \ldots, \tau_L) \propto P(\tau_1, \tau_2) P(\tau_2, \tau_3) \cdots P(\tau_{L-1}, \tau_L) P(\tau_L, \tau_1). \tag{12}$$

The 3-cluster approximation is depicted graphically in Figure 2c.

In general, the master equation in n-cluster approximation leads to $(v_{\max}+1)^n$ nonlinear equations. This number can be reduced by using the so-called Kolmogorov consistency conditions [15]

$$\begin{aligned} \sum_{\tau=0}^{v_{\max}} P(\tau_1, \ldots, \tau_{n-1}, \tau) &= P(\tau_1, \ldots, \tau_{n-1}) \\ &= \sum_{\tau=0}^{v_{\max}} P(\tau, \tau_1, \ldots, \tau_{n-1}). \end{aligned} \tag{13}$$

Nevertheless, a solution is only feasible for relatively small cluster-sizes [6]. The quality of the approximation improves with increasing n and for $n \to \infty$ the n-cluster result becomes exact.

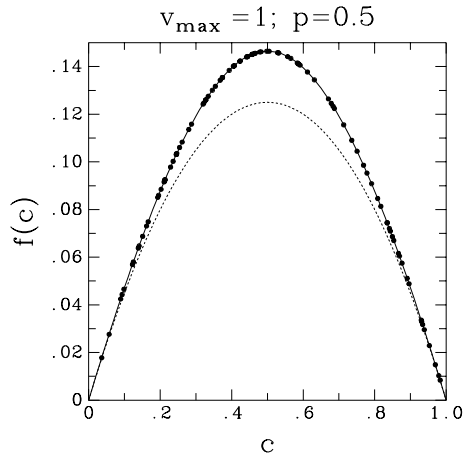

Fig. 3. Fundamental diagram for $v_{\max} = 1$: Comparison of computer simulations (•) with the exact solution (full line) and the mean-field result (broken line).

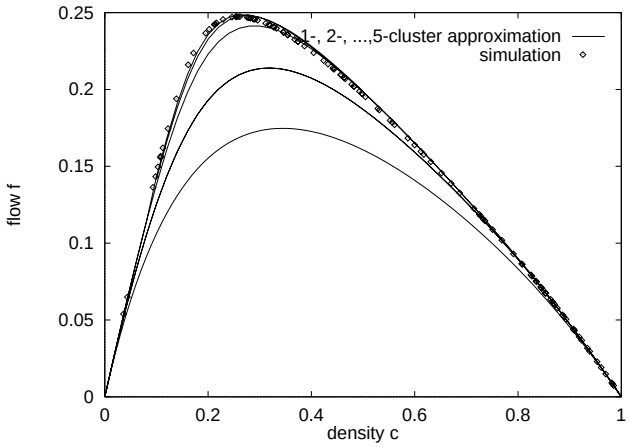

Fig. 4. Comparison of simulation results with the n-cluster approximation ($n = 1, \ldots, 5$ from bottom to top) for the fundamental diagram for $v_{\max} = 2$ and $p = 1/2$.

However, for $v_{\max} = 1$ already the 2-cluster approximation is exact [5,6]. The 2-cluster probabilities for the stationary state are given explicitly by

$$\begin{aligned} P(0,0) &= 1 - c - P(1,0), \\ P(1,1) &= c - P(1,0), \\ P(1,0) &= P(0,1) = \frac{1}{2\bar{p}} \left[1 - \sqrt{1 - 4\bar{p}c(1-c)}\right], \end{aligned} \tag{14}$$

where again $\bar{p} = 1-p$. The flow is given by $f(c) = \bar{p}P(1,0)$.

Higher order cluster approximations with $n > 2$ yield the same result (14). This indicates that (14) is exact. Indeed this has been proven in [6] by a combinatorial argument.

For $v_{\max} = 2$ already the 2-cluster approximation yields a nonlinear system of equations which has to be solved numerically. The fundamental diagrams obtained from the n-cluster approximation ($n = 1, \ldots, 5$) are compared in Figure 4 with results of Monte Carlo simulations. One can see a rapid convergence and already for $n = 4$ the difference between the simulation and the cluster result is extremely small.

3.3 Car-oriented mean-field theory

The car-oriented mean-field (COMF) theory [7] is another possibility to take into account correlations in an analytical description[2].

The rules R1–R4 can be rewritten in terms of d_j and v_j only. Therefore the state of the system can be characterized instead of the occupation numbers τ_j equivalently by the headways and the velocities[3]. The central quantity in COMF is the probability $P_n(v)$ to find exactly n empty cells (*i.e.* a gap of size n) in front of a car with velocity v. In this way certain longer-ranged correlations are already taken into account. The essence of COMF is now to neglect correlations between the headways.

Using again the update ordering R2-R3-R4-R1 (see Sect. 3.2), one obtains for $v_{\max} = 1$ the following system of equations resulting from the master equation for the stationary state (with $P_n = P_n(v = 1)$):

$$\begin{aligned} P_0 &= \bar{g}\left[P_0 + \bar{p}P_1\right], \\ P_1 &= gP_0 + \left[\bar{p}g + p\bar{g}\right]P_1 + \bar{p}\bar{g}P_2, \\ P_n &= pgP_{n-1} + \left[\bar{p}g + p\bar{g}\right]P_n + \bar{p}\bar{g}P_{n+1}, \quad (n \geq 2) \end{aligned} \tag{15}$$

where $g = \bar{p}\sum_{n\geq 1} P_n = \bar{p}[1 - P_0]$ is the probability that a car moves in the next timestep. $\bar{g} = 1 - g$ then is the probability that a car does not move.

As an example for the derivation of these equations we consider the equations for $n \geq 2$. Since the velocity difference of two cars is at most 1, a gap of n cells at time $t + 1$ must have evolved form a gap of length $n - 1$, n, or $n + 1$ in the previous timestep. A headway of $n - 1$ cells evolves into a headway of n cells only if the first car moves (with probability g) and the second car brakes in the randomization step (probability p), *i.e.* the total probability for this process is pgP_{n-1}. Similarly, the headway remains constant only if either both cars move (probability $\bar{p}g$) or both cars do not move (probability $p\bar{g}$). Finally, the headway is reduced by one, if only the second car moves (probability $\bar{p}\bar{g}$).

The probabilities P_n have to satisfy the normalization conditions

$$1 = \sum_{n=0}^{\infty} P_n, \tag{16}$$

$$\frac{1}{c} = \sum_{n=0}^{\infty} (n+1)P_n. \tag{17}$$

(17) is a consequence of the conservation of the number of cars since each car with headway n occupies $n + 1$ cells.

[2] A similar method for reaction-diffusion models is discussed in [18].

[3] For a complete equivalence one has to track the position x_1 of one car, *e.g.* car 1. From x_1, $\{d_j\}$ and $\{v_j\}$ one can then determine $\{\tau_j\}$.

Although the infinite system of non-linear equations (15) looks more difficult than those of the cluster approximation, a solution possible using generating functions [7]. For $v_{\max} = 1$ one finds

$$P_0 = \frac{1}{2\bar{p}c}\left[2\bar{p}c - 1 + \sqrt{1 - 4\bar{p}c(1-c)}\right],$$
$$P_n = \frac{P_0}{p}\left(\frac{p(1-P_0)}{P_0 + p(1-P_0)}\right)^n \quad (n \geq 1), \qquad (18)$$

and for the flow $f(c,p) = cg$ again the exact solution is reproduced.

For $v_{\max} = 2$ one has two coupled systems of the type (15), since one has to distinguish $P_n(v = 1)$ and $P_n(v = 2)$ and the probabilities g_α that a car moves $\alpha = 0, 1, 2$ cells in the next timestep. This system has a similar structure as (15) and is given explicitly in [7]. It can also be solved, but does not give the exact solution.

Note that the COMF approach assumes an infinite system size. For a finite system of length L the largest headway that can appear is $M := L - N$. For $v_{\max} = 1$ it is possible to satisfy (16) and (17) by just changing the equations for P_{M-1} and P_M:

$$P_{M-1} = pgP_{M-2} + [\bar{p}g + p\bar{g}]\,P_{M-1} + [\bar{p}\bar{g} - pg]\,P_M,$$
$$P_M = pgP_{M-1} + [1 - \bar{p}\bar{g} + pg]\,P_M. \qquad (19)$$

The equations for P_n with $n < M - 1$ are the same as in (15). In order to derive (19) we have made the Ansatz $P_{M-1} = \alpha_1 P_{M-2} + \alpha_2 P_{M-1} + \alpha_3 P_M$ and $P_M = \beta_1 P_{M-1} + \beta_2 P_M$ and determined the coefficients α_j and β_j from (16) and (17).

For $v_{\max} = 2$ it appears that the equations for all n have to be modified in order to satisfy (16, 17). This corresponds nicely to the qualitative difference of the cases $v_{\max} = 1$ and $v_{\max} > 2$ and the appearance of long-ranged correlations in the latter (see Sect. 3.4).

3.4 Garden of eden states

An important effect of the parallel dynamics is the existence of configurations which can not be reached dynamically [8]. These states are called Garden of Eden (GoE) states or paradisical states since one never gets back once one has left [19]. An example for a GoE state is given in Figure 5. Note that the velocity is equal to the number of cells that the car moved in the previous timestep. For the configuration shown in Figure 5 this implies that the two cars must have occupied the same cell before the last timestep. Since this is forbidden in the NaSch model, the configuration shown can never be generated by the dynamics.

The simple mean-field theory presented in the previous section does not take into account the existence of GoE states. One can therefore hope that by eliminating all GoE states and applying mean-field theory in the reduced configuration space (paradisical mean-field, pMF) one will find a considerable improvement of the MF results.

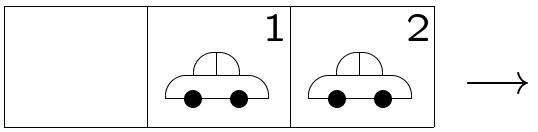

Fig. 5. A Garden of Eden state for the model with $v_{\max} \geq 2$.

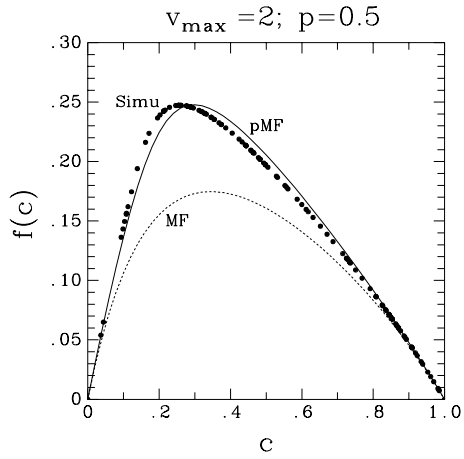

Fig. 6. Comparison of the fundamental diagrams obtain from MC simulations with the results of mean-field theory (MF) and mean-field theory without GoE states (paradisical mean-field, pMF).

For $v_{\max} = 1$ all states containing the local configurations $(0,1)$ or $(1,1)$ are GoE states, *i.e.* the cell behind a car with velocity 1 must be empty[4]. This only affects equation (1) and the equations for pMF theory read:

$$c_0 = \mathcal{N}(c_0 + pd)c, \qquad (20)$$
$$c_1 = \mathcal{N}\bar{p}cd, \qquad (21)$$

where the normalization $\mathcal{N}$ ensures $c_0 + c_1 = c$ and is given explicitly by $\mathcal{N} = 1/(c_0 + d)$.

Solving (21) for c_1 by using $c_0 = c - c_1$, one obtains c_1 as a function of the density c:

$$c_1 = \frac{1}{2}\left(1 - \sqrt{1 - 4\bar{p}(1-c)c}\right) \qquad (22)$$

(with $\bar{p} = 1 - p$). Since the flow is given by $f(c) = c_1$ we recover the exact solution for the case $v_{\max} = 1$ (see Sect. 3.2).

It is interesting to note that for random-sequential dynamics MF theory is exact whereas for parallel dynamics pMF is exact. Therefore the origin of the correlations is the parallel update procedure. The existence of the GoE states is responsible for the differences between parallel and random-sequential dynamics. This is probably not only true for the NaSch model, but is a rather general property of CA models.

For $v_{\max} = 2$ one has to take into account more GoE states [8]. pMF is no longer exact, but it still leads to a considerable improvement of the MF results (see Fig. 6).

[4] Here we do not use the changed update order, so "0" denotes a cell occupied by a car with velocity 0.

4 "Physical" quantities

In this section we will use the analytical methods of Section 3 to determine physical quantities of the NaSch model, *e.g.* the fundamental diagram, cluster-size distributions and correlation functions. These results will be used in Section 5 to gain a better understanding of the microscopic structure of the stationary state.

4.1 Fundamental diagram

For $v_{\max} = 1$ the fundamental diagram in MF approximation is given by

$$f_{\mathrm{MF}}(c) = \bar{p}c(1-c). \tag{23}$$

As already mentioned in this case 2-cluster approximation, COMF and pMF are exact and the flow is given

$$f(c,p) = \frac{1}{2}\left(1 - \sqrt{1 - 4\bar{p}(1-c)c}\right) \tag{24}$$

(with $\bar{p} = 1-p$). The fundamental diagram is symmetric with respect to $c = 1/2$, reflecting the particle-hole symmetry of the NaSch model with $v_{\max} = 1$.

It is apparent from Figure 3 that MF considerably underestimates the flow for intermediate densities. This shows that correlations are important in this regime. These correlations lead to an increase of the flow. One finds a particle-hole attraction (particle-particle repulsion), *i.e.* the probability to find an empty site in front of a car is enhanced compared to a completely random configuration. In terms of cluster probabilities this particle-hole attraction can be expressed more quantitatively as $P(1,0) > P(1)P(0) = c(1-c)$.

As mentioned in Section 3.4, pMF yields the exact solution for $v_{\max} = 1$. This shows that there are no "true" correlations apart from those due to the existence of GoE states. The 2-cluster approximation and COMF then become exact since both methods are able to identify all GoE states.

For $v_{\max} > 1$ one expects stronger correlations than for $v_{\max} = 1$ [6]. Indeed for $v_{\max} = 2$ the difference between the MF prediction

$$f_{\mathrm{MF}}(c) = c_1 + 2c_2 = \frac{\bar{p}(1+\bar{p}d^2)dc}{1-pd^2} \tag{25}$$

and the Monte Carlo data is even larger (see Fig. 4). However, pMF is not exact and therefore "true" correlations exist. This is in agreement with the fact that MF is also not exact for the NaSch model with $v_{\max} > 1$ and random-sequential dynamics.

The correlations can be taken into account systematically by the $n-$cluster approach which converges rapidly with increasing n. Already for $n = 4$ one obtains a very good agreement with the simulation results (Fig. 4). The quality of COMF depends strongly on the value of p. In general its prediction is between the 2– and 3–cluster approximation.

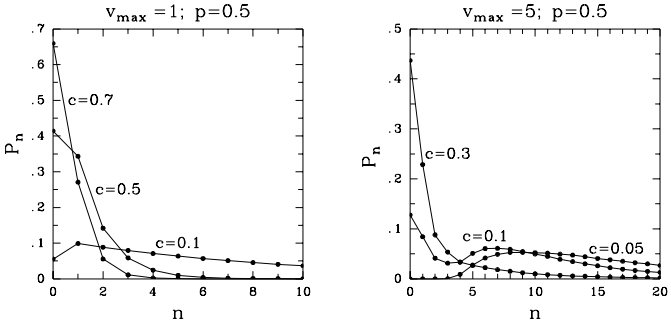

Fig. 7. Distribution of headways for different densities for $v_{\max} = 1$ and $p = 0.5$ (left) and $v_{\max} = 5$ and $p = 0.5$ (right).

4.2 Headway distribution

Figure 7 shows the result for the distribution of headways, P_n, for $v_{\max} = 1$. Since in this case COMF is exact, we can use the result (18). The headway distribution has just one maximum, located at $n = 1$ for small densities and at $n = 0$ for large c.

These two regimes also exist for higher velocities. At high densities the headway distribution is maximal at $n = 0$, whereas for low densities the maximum is found at some value $n_{\max} > 0$, where $n_{\max}$ depends on the density. In addition, an intermediate density regime exists, where distribution exhibits two local maxima, one at $n = 0$, corresponding to jammed cars, and one at $n_{\mathrm{loc}} > 0$, corresponding to free flowing cars [20].

4.3 Correlation length

As an application of the cluster approximation we will compute density-density correlations for $v_{\max} = 1$ in the following. Using occupation numbers $n_j = 0, 1$ the density-density correlation function is defined by

$$\langle n_1 n_r \rangle = {\sum_{\{n_j\}}}' n_1 n_r P(n_1, \ldots, n_L) \tag{26}$$

where the prime indicates that the sum runs over all states with fixed particle number $N = n_1 + \cdots + n_L$.

In order to evaluate the sum in (26), it is convenient to use a grand-canonical description. One introduces a fugazity z which controls the average number of particles $\langle n_j \rangle$ and sums over all configurations in (26). Using the 2-cluster approximation (12) – which is exact for $v_{\max} = 1$ – the correlation function is given by

$$\langle n_1 n_r \rangle = \frac{1}{Z_{gc}} \sum_{\{n_j\}} n_1 n_r z^N P(n_1, n_2) P(n_2, n_3) \cdots \cdots P(n_{L-1}, n_L) P(n_L, n_1) \tag{27}$$

with $N = \sum_{j=1}^{L} n_j$ and the normalization

$$Z_{gc} = \sum_{\{n_j\}} z^N \prod_{j=1}^{L} P(n_j, n_{j+1}). \tag{28}$$

Introducing the transfer matrix

$$\tilde{\mathbf{P}} = \begin{pmatrix} P(0,0) & \sqrt{z}P(0,1) \\ \sqrt{z}P(1,0) & zP(1,1) \end{pmatrix} \tag{29}$$

this can be written succinctly as

$$Z_{gc} = \mathrm{Tr}\ \tilde{\mathbf{P}}^L, \tag{30}$$

$$\langle n_1 n_r \rangle = \frac{1}{Z_{gc}} \mathrm{Tr} \left(\mathbf{Q}\tilde{\mathbf{P}}^{r-1}\mathbf{Q}\tilde{\mathbf{P}}^{L-r+1} \right), \tag{31}$$

with the matrix $\mathbf{Q}(n_1, n_2) = n_1 \tilde{\mathbf{P}}(n_1, n_2)$.

The correlation length ξ can be obtained from the asymptotic behaviour ($r \to \infty$) of the correlation function

$$\langle n_1 n_r \rangle - c^2 \propto \mathrm{e}^{-r/\xi} \tag{32}$$

where $c = \langle n_j \rangle$ is the (average) density of cars. ξ is determined by the ratio of the eigenvalues $\lambda_\pm$ of $\tilde{\mathbf{P}}$ (with $|\lambda_+| \geq |\lambda_-|$):

$$\xi^{-1} = \ln \left| \frac{\lambda_-}{\lambda_+} \right|. \tag{33}$$

The explicit expression for ξ can be obtained from

$$\lambda_\pm = \frac{1}{2} \left[A \pm \sqrt{A^2 + 4\bar{p}z[P(1,0)]^2} \right], \tag{34}$$

$$\text{with} \quad A = P(0,0) + zP(1,0). \tag{35}$$

$P(a,b)$ are the cluster probabilities given in (14). The fugazity z can be related to the density c *via* the equation $c = \langle n_j \rangle$. Using an expression analogous to (31) one finds

$$c\lambda_+ = \frac{B\left\{[P(1,0)]^2 + BP(1,1)\right\}}{[P(1,0)]^2 + \frac{1}{z}B^2}, \tag{36}$$

$$\text{with} \quad B = \lambda_+ - P(0,0). \tag{37}$$

For fixed p, ξ is maximal for $c = 1/2$ which corresponds to $z = 1$. $\xi(c = 1/2)$ diverges only for $p \to 0$. In that case one finds that $\xi(c = 1/2) \propto p^{-1/2}$. Monte Carlo simulations show that the same behaviour still occurs (at density $c = 1/(v_{\max}+1)$) for $v_{\max} > 1$ [21]. Therefore, the correlation function already gives an indication that the system is not critical for $p > 0$. The simulations show that there is no qualitative difference between the cases $v_{\max} = 1$ and $v_{\max} > 1$ as far as the phase transition is concerned [21].

The above results demonstrate that, although the 2-cluster approximation is exact, not all correlation functions are of finite range.

4.4 Jam-size distribution

For a better understanding of the differences between the cluster approximation and COMF we calculate the distribution of jam-sizes using these methods. Let C_n be the probability to find a (compact) jam of length n, *i.e.* n consecutive occupied cells.

In COMF, C_n is proportional to $(1-P_0)P_0 \cdots P_0(1-P_0) = (1-P_0)^2 P_0^{n-1}$. The number of jams is proportional to $1 - P_0$ so that one finds

$$C_n = (1-P_0)P_0^{n-1}. \tag{38}$$

This distribution is purely exponential and $P_n \geq P_{n+1}$ for all n. Therefore COMF is not able to describe clustering or phase separation, *i.e.* situations where jams with more than one car dominate. Clustering implies that there are correlations between gaps which are completely neglected in COMF.

In 2-cluster approximation, C_n is proportional to $P(\underline{0}|1)P(\underline{1}|1)\cdots P(\underline{1}|1)P(\underline{1}|1)P(\underline{1}|0)$ where we have used the conditional probabilities (10). and the different update-ordering R2-R3-R4-R1. Note that the case $n = 1$ has to be treated separately, $C_1 \propto \sum_{v=1}^{v_{\max}} P(\underline{0}|v)P(\underline{v}|0)$. The number of jams is obviously given by $\mathcal{N}_J = \sum_{v=1}^{v_{\max}} P(\underline{v}|0)$ and one obtains

$$C_n^{(2)} = \frac{1}{\mathcal{N}_J} P(\underline{0}|1)P(\underline{1}|1)^{n-2}P(\underline{1}|1)P(\underline{1}|0) \quad (n \geq 2),$$

$$C_1^{(2)} = \frac{1}{\mathcal{N}_J} \sum_{v=1}^{v_{\max}} P(\underline{0}|v)P(\underline{v}|0). \tag{39}$$

$C_n^{(2)}$ decays exponentially for $n \geq 2$, especially one has $C_{n+1} \leq C_n$. For the m-cluster approximation one can derive similar expressions. Since here clusters of size m are treated exactly it is now possible to find the maximum of the jam-size distribution somewhere between $n = 1$ and $n = m$. For $n > m$ the jam-size probability decays exponentially due to the mean-field-like self-consistent coupling of the cluster to the rest of the system.

4.5 Further applications

We briefly mention other results which have been obtained analytically using the cluster approximation. In [20] the distributions of gaps and the distance between jams have been calculated for $v_{\max} = 1$ using the 2-cluster approximation. For the gap distribution one recovers the (exact) result which has been derived in Section 3.3 (see Eq. (18)). For the calculation of the distribution of gaps between jams one defines every vehicle with velocity 0 to be jammed. The distance between two jams is then given by the distance between a car with velocity 0 and the next car with velocity 0. In [22] the probability $\mathcal{P}(t)$ of a time headway t has been investigated. This quantity is defined in analogy to measurements on real traffic where a detector registers the time interval between the passing of consecutive cars. For a discussion of the behaviour of the time-headway and the jam-gap distribution in the NaSch model we refer to [20,22]. These quantities are also very useful for studying variants of the NaSch model which exhibit phase separation [23].

5 Microscopic structure of the stationary state

In the following we demonstrate that the microscopic structure of the stationary state changes qualitatively with the braking parameter p. For illustration we first discuss the deterministic limits $p = 0$ and $p = 1$. After that the behaviour for randomizations $0 < p < 1$ is discussed. However, we concentrate on the limits $p \ll 1$ and $1 - p \ll 1$. Finally, in Section 5.4 we compare COMF and cluster approximation. Here we focus on the ability to reproduce the correct microscopic structure of the stationary state.

5.1 p = 0

In the absence of random decelerations the velocity of the vehicles is determined solely by its headway. For densities $c \leq 1/(v_{\max}+1)$ all headways can be larger than $v_{\max}$ and therefore the cars move with velocity $v_{\max}$ in the stationary state. This is no longer possible for $c > 1/(v_{\max}+1)$. Here the velocity of the cars is determined by the average headway $\bar{d}$ available, $\bar{d} = (L-N)/N = (1-c)/c$. The fundamental diagram is therefore given by

$$f(c) = \begin{cases} v_{\max} c & \text{for } c \leq 1/(v_{\max}+1), \\ 1-c & \text{for } c > 1/(v_{\max}+1). \end{cases} \tag{40}$$

Note that in general the stationary state is not unique, but determined completely by the initial condition.

For $p = 0$ there is no tendency towards clustering [24]. Overreactions are not possible and there is no spontaneous formation of jams. In this sense the case $p = 0$ is unrealistic. The dynamics is completely determined by "geometrical" effects, since the behaviour of the cars only depends on the available average headway. There is no "attractive" interaction between the cars and therefore no mechanism for clustering.

5.2 p = 1

In the case $p = 1$ the dynamics is again deterministic. However, it is very different from that of a model with maximum velocity $v_{\max} - 1$. The point that we want to stress here is the existence of metastable states. For $v_{\max} = 2$ and density $c = 1/3$ the state ..1..1..1.. (here "." denotes an empty cell and "1" a cell occupied by a car with velocity 1) is stationary with flow $f(c = 1/3) = 1/3$. On the other hand, the state ..0..0..0.. is also stationary with vanishing flow, since a standing car will never start to move for $p = 1$.

For densities $c > 1/3$ all stationary states have vanishing flow. Here at least one car has only one empty cell in front. Therefore after step R2 this car has velocity 1 and will then decelerate to velocity 0 in step R3. After that it will never move again.

For densities $c \leq 1/3$ stationary states with non-zero flow exist. These are not stable under local perturbations, *i.e.* stopping just one car leads to a complete breakdown of the flow. In this sense these states are metastable.

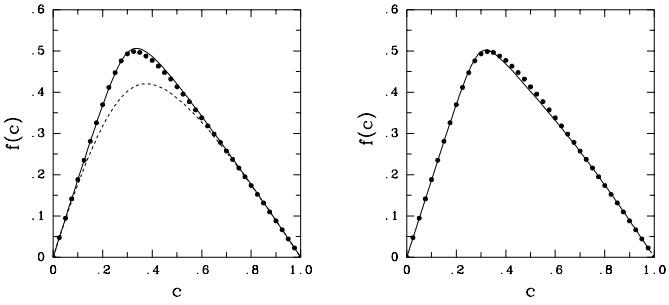

Fig. 8. Fundamental diagram for $v_{\max} = 2$ and $p = 0.1$: Comparison of simulation data (•) with the 2-cluster ($\cdots$) and 3-cluster results (—) (left) and with COMF (—) (right).

Starting from random initial conditions, the metastable states have a vanishing weight in the thermodynamic limit, since already one standing car leads to a zero-flow state.

Note that the metastable states at $p = 1$ do not exist for $v_{\max} = 1$. In that sense the difference between $v_{\max} = 1$ and $v_{\max} > 1$ becomes most pronounced at $p = 1$.

The deceleration introduces a kind of "attractive" interaction between the cars which can lead to the formation of jams. However, these jams are typically not compact, but of the form .0.0.0.0.. A car approaching a standing car adapts its velocity in step R2 such that it reaches the cell just behind the standing vehicle. In step R3 it then decelerates further and so there will be a gap of 1 between the cars.

5.3 0 < p < 1

In the limit $p \to 0$, the fundamental diagrams obtained from COMF and the 3-cluster approximation become exact, in contrast to the 2-cluster approximation (see Fig. 8). Even for values of $p \approx 0.1$ there is an excellent agreement between the fundamental diagrams obtained analytically and the Monte Carlo simulations. Since "realistic" values of p are in the region $p \sim 0.1 - 0.2$, the approximations are indeed applicable in the relevant parameter regime.

Figure 9 shows a comparison of the computer simulations with the COMF results for the probabilities g_α that a car moves α sites. Although there is an excellent agreement for the fundamental diagram $f(c) = c(g_1 + 2g_2)$ at $p = 0.1$ (see Fig. 8), there are considerable deviations at intermediate densities for the individual values of g_1 and g_2. This is somewhat surprising and indicates that COMF is not exact in the limit $p \to 0$, *i.e.* that there are still correlations between the headways. This will be discussed further in Section 5.4.

On the other hand, the 3-cluster probabilities obtained from our simulations show a very good agreement with the results of the 3-cluster approximation (Fig. 10). This suggests that the 3-cluster approximation is asymptotically exact for $p \to 0$.

The limit $p \to 1$ is difficult to investigate numerically. Preliminary results show that COMF is not exact in this limit. The cluster approximations give a much better agreement with Monte Carlo simulations, but it is not

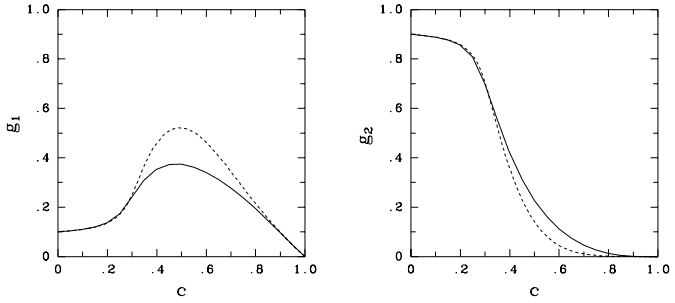

Fig. 9. Comparison of the COMF prediction ($\cdots$) with computer simulations (—) for the probabilities g_α that a car moves α sites. g_0 can be obtained from $g_0 = 1 - g_1 - g_2$. The braking parameter is $p = 0.1$ and $v_{\max} = 2$.

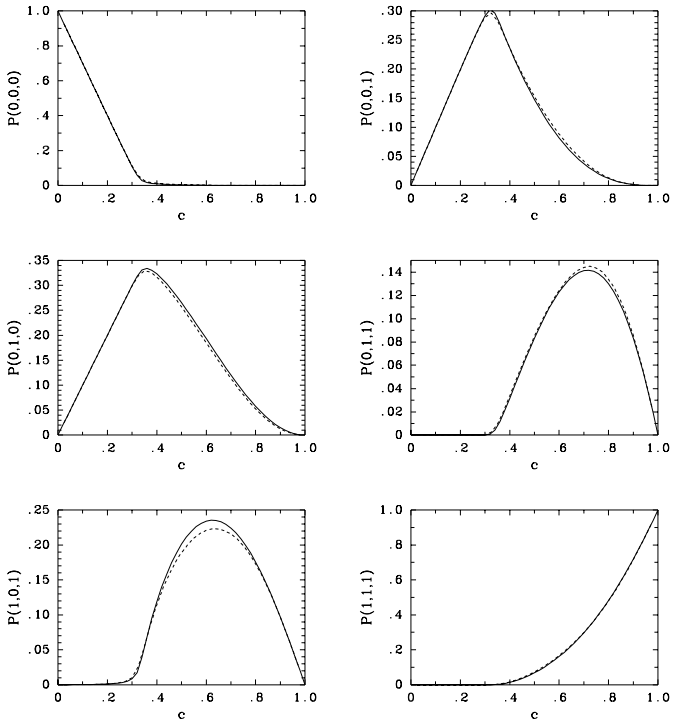

Fig. 10. Comparison of the 3-cluster probabilities $P(n_j, n_{j+1}, n_{j+2})$ obtained from computer simulations (—) and the 3-cluster approximation ($\cdots$) for $p = 0.01$. n_j is the occupation number of cell j. Note that $P(1,0,0) = P(0,0,1)$ and $P(1,1,0) = P(0,1,1)$.

clear yet whether it becomes exact or not. However one can expect a tendency towards phase seperation due to "attractive" interactions beween the cars. One stopped car can induce jams with a rather long lifetime since the restart probability of the first car is rather small. This tendency can already be observed in the cluster probabilities for $p = 0.75$ (see Fig. 11). The distributions become broader and especially at small densities the probabilities $P(0,1,1)$ and $P(1,1,1)$ which characterize the clustering are enhanced compared to the limit $p \to 0$.

5.4 Cluster approximation vs. COMF

In this section the results of the cluster approximation and COMF in special limits are compared. As already

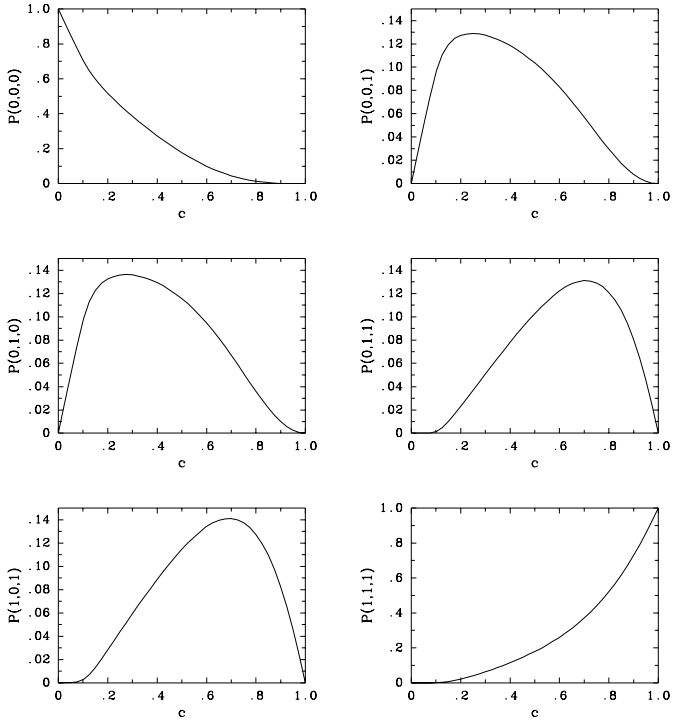

Fig. 11. Same as Figure 10, but for $p = 0.75$. Here only the results of the computer simulations are shown.

mentioned, both methods yield the exact solution for $v_{\max} = 1$. This is related to the fact that paradisical mean-field is exact in that case and both methods are able to identify all GoE states. For $v_{\max} = 2$ the situation is different. Here all three methods are only approximative.

The deviations between COMF results and the Monte Carlo simulations can be understood by looking more closely at the microscopic structure of the stationary state. For $p = 0$ there are three different stable structures: 00000, .1.1.1., and ..2..2....2...2.... The last structure comprises all configurations where all cars have velocity $v_{\max}$ and at least $v_{\max}$ empty cells in front. For fixed density there are many configurations which produce the same flux. In a large system these configurations are mostly made up of combinations of the three stable structure (with small transition regions). For $p > 0$, .1.1.1. is the most unstable configuration. It tends to separate into 00000 and 2..2....2...2 under fluctuations of the headways. COMF is not able to account for these fluctuations since headways are assumed to be independent. Therefore the weight of the configurations .1.1.1. – and therefore g_1 – is overestimated. In the 3-cluster approach, on the other hand, the headways are not independent. Therefore it is able to identify the dominating local structure for $p \to 0$ correctly.

COMF is not able to describe the "attractive" part of the interaction properly. This can also be seen in the jam-size distribution (see Sect. 4.4). COMF always predicts a strictly monotonous distribution (38), whereas the cluster approximation in principle is able to describe situations where the jam-size distribution has a maximimum at some (small) value of $n > 0$.

6 Summary

Although cellular automata are designed for efficient computer simulation studies, an analytical description is possible, although difficult. We have presented here four different methods which can be applied to CA models of traffic flow. The first approach, a simple mean-field theory for cell occupation numbers, is insufficient since the important correlations between neighbouring cells (*e.g.* the particle-hole attraction) are neglected. We therefore suggested three different improved mean-field theories. These approaches take into account certain correlations between the cells. The simplest method is the so-called "paradisical mean-field" theory which is based on the observation that certain configurations (Garden of Eden states) can never be generated by the dynamical rules due to the use of parallel dynamics. The cluster approximation, on the other hand, treats clusters of a certain size exactly and couples them in a self-consistent way. Therefore short-ranged correlations are taken into account properly. In contrast, car-oriented mean-field theory is a true mean-field theory, but here one uses a different dynamical variable, namely the distance between consecutive cars. In that way, certain correlations between cells are taken into account.

All three improved MF theories become exact for $v_{\max} = 1$. For larger values of $v_{\max}$ they are just approximations. In principle, the cluster approximation and COMF (in combination with a cluster approach) can be improved systematically. This is, however, very cumbersome.

An interesting observation is that the quality of the approximation depends strongly on the value of p. This indicates that the physics changes with p, contrary to common believe. Evidence for this scenario comes from the microscopic structure of the stationary state. In the limit $p \to 0$ it is dominated by repulsive interactions which tend to align the vehicles at a headway of at least $v_{\max}$ cells. On the other hand, for $p \to 1$ there is a tendency towards phase seperation. Cars which had to stop due to a fluctuation will stand for a rather long time and thus lead to the creation of jams. In the deterministic case this even leads to the existence of metastable states.

In [25] it has been suggested that the behaviour of the NaSch model is governed by two fixed points, namely $p = 0$ and $v_{\max} = \infty$. Our investigations show that it might be more reasonable to consider $p = 0$ and $p = 1$ as fixed points in order to understand the behaviour for fixed $v_{\max}$. For $p = 0$ there is a continuous phase transition from laminar flow to a congested phase (see [21,25] and references therein) at $c = 1/(v_{\max} + 1)$. This transition turns into a crossover at $0 < p < 1$ [21,25]. It would be desirable to investigate the behaviour of this transition close to $p = 1$ in more detail.

The methods presented here can also be used for other CA models, *e.g.* variants of the NaSch model [22,23,26–29]. The investigation of the NaSch model has led to a better understanding of their advantages and limitations so that it is easier to choose the approach most suitable for a given problem.

I would like to thank Michael Schreckenberg, Ludger Santen, Debashish Chowdhury and Dietrich Stauffer for valuable discussions and useful suggestions. This work has been performed within the research program of the SFB 341 (Köln–Aachen–Jülich).

References

1. S. Wolfram, *Theory and Applications of Cellular Automata* (World Scientific, Singapore 1986).
2. *Traffic and Granular Flow*, edited by D.E. Wolf, M. Schreckenberg, A. Bachem (World Scientific, Singapore, 1996).
3. *Traffic and Granular Flow '97*, edited by M. Schreckenberg, D.E. Wolf (Springer, 1998).
4. K. Nagel, M. Schreckenberg, J. Phys. I France **2**, 2221 (1992).
5. A. Schadschneider, M. Schreckenberg, J. Phys. A: Math. Gen. **26**, L679 (1993).
6. M. Schreckenberg, A. Schadschneider, K. Nagel, N. Ito, Phys. Rev. E **51**, 2339 (1995).
7. A. Schadschneider, M. Schreckenberg, J. Phys. A: Math. Gen. **30**, L69 (1997).
8. A. Schadschneider, M. Schreckenberg, J. Phys. A: Math. Gen. **31**, L225 (1998).
9. L.G. Tilstra, M.H. Ernst, J. Phys. A: Math. Gen. **31**, 5033 (1998).
10. A.B. Kolomeisky, G. Schütz, E.B. Kolomeisky, J.P. Straley, J. Phys. A: Math. Gen. **31**, 6911 (1998).
11. M. Rickert, K. Nagel, M. Schreckenberg, A. Latour, Physica A **231**, 534 (1996).
12. D. Chowdhury, A. Schadschneider, Phys. Rev. E **59**, R1311 (1999).
13. R. Barlovic, L. Santen, A. Schadschneider, M. Schreckenberg, Eur. Phys. J. B **5**, 793 (1998).
14. R. Kikuchi, Prog. Theor. Phys. Suppl. **35**, 1 (1966),
15. H.A. Gutowitz, J.D. Victor, B.W. Knight, Physica D **28**, 18 (1987).
16. D. ben-Avraham, J. Köhler, Phys. Rev. A **45**, 8358 (1992).
17. A. Crisanti, G. Paladin, A. Vulpiani, *Products of Random Matrices in Statistical Physics* (Springer, Berlin, 1993).
18. D. ben-Avraham, in *Nonequilibrium Statistical Mechanics in One Dimension*, edited by V. Privman (Cambridge University Press, 1997).
19. E.F. Moore, Proc. Symb. Appl. Math. **14**, 17 (1962).
20. D. Chowdhury, K. Ghosh, A. Majumdar, S. Sinha, R.B. Stinchcombe, Physica A **246**, 471 (1997).
21. B. Eisenblätter, L. Santen, A. Schadschneider, M. Schreckenberg, Phys. Rev. E **57**, 1309 (1998).
22. K. Ghosh, A. Majumdar, D. Chowdhury, Phys. Rev. E **58**, 4012 (1998).
23. D. Chowdhury, L. Santen, A. Schadschneider, S. Sinha, A. Pasupathy, J. Phys. A: Math. Gen. **32**, 3229 (1999).
24. K. Nagel, H.J. Herrmann, Physica A **199**, 254 (1993).
25. M. Sasvari, J. Kertész, Phys. Rev. E **56**, 4104 (1997).
26. A. Schadschneider, M. Schreckenberg, Ann. Physik **6**, 541 (1997).
27. B.-W. Wang, Y.-R. Kwong, P.-H. Hui, Phys. Rev. E **57**, 2568 (1998).
28. B.-H. Wang, L. Wang, P.M. Hui, B. Hu, Phys. Rev. E **58**, 2876 (1998).
29. A. Schadschneider, in [3].